

Effect of multispin interactions on spin dynamics in the Néel state of La_2CuO_4

Luca Capriotti,¹ Andreas Läuchli,² and Arun Paramekanti³

¹Valuation Risk Group, Credit Suisse First Boston (Europe) Ltd.,
One Cabot Square, London E14 4QJ, United Kingdom

²Institut Romand de Recherche Numérique en Physique des Matériaux (IRRMA), PPH-Ecublens, CH-1015 Lausanne

³Department of Physics, University of California, Berkeley 94720-7300, U.S.A.

We use Schwinger boson mean field theory to study the effect of four-spin interactions on spin dynamics in the Néel state of La_2CuO_4 . An accurate fit of the magnon dispersion relation, measured by Coldea *et al.* [Phys. Rev. Lett. **86**, 5377 (2001)] is obtained with Hubbard model parameters $U \approx 2.34\text{eV}$, and $t \approx 360\text{meV}$. These parameters lead to estimates of the staggered magnetization ($m_s \approx 0.285$), spin wave velocity ($c \approx 800\text{meV}\text{-}\text{\AA}$), and spin stiffness ($\rho_s \approx 24\text{meV}$) consistent with experimental findings. The dynamical structure factor shows considerable weight in the continuum along the zone boundary as well as secondary peaks that could be observed in high resolution neutron scattering experiments.

PACS numbers: 75.10.Jm, 75.40.Gb, 71.10.Fd, 75.30.Ds

I. INTRODUCTION

Multispin interactions are important in a variety of magnetic systems.¹ In a magnetically ordered insulator, such interactions can reveal themselves through their effect on the spin dynamics measured in neutron scattering experiments. One system which appears to provide an example of such physics is La_2CuO_4 , which is a Mott insulating antiferromagnet. Indeed, high resolution data on the magnon dispersion in this system indicate a dip in the magnon energy near $\mathbf{Q} = (\pi/2, \pi/2)$ while traversing the magnetic Brillouin zone boundary along $(\pi, 0) \rightarrow (0, \pi)$. Such a dip is not expected for the magnon dispersion in a nearest-neighbor Heisenberg antiferromagnet, but it has been suggested² that it could arise from the four-spin interactions due to ring-exchange processes which appear naturally when local charge fluctuations in the Mott insulator are taken into account. Motivated by this, we revisit the zero temperature spin dynamics in the Néel ordered state of La_2CuO_4 .

La_2CuO_4 is a layered antiferromagnet. While the exchange coupling between the two-dimensional layers is crucial for the existence of a finite-temperature Néel transition in this system, this interplane coupling is nevertheless tiny in magnitude, $\sim 10^{-5}$ of the in-plane exchange coupling, and much smaller than the resolution of the neutron scattering experiments. It is therefore expected that the low temperature spin dynamics in the Néel ordered state in this material is adequately captured by the Hubbard model at zero temperature on a two dimensional square lattice, (with standard notations)

$$H = -t \sum_{\langle ij \rangle, \sigma} \left(c_{i\sigma}^\dagger c_{j\sigma} + h.c. \right) + U \sum_i n_{i\uparrow} n_{i\downarrow} \quad (1)$$

in its insulating phase at strong coupling $U \gg t$. In this regime, it is well known³ that the low energy physics can be encapsulated in an effective spin Hamiltonian which incorporates two-spin and four-spin interactions (given below in Eq. 2).

In this paper, we use Schwinger boson mean field theory to study the magnon dispersion and scattering continuum for this effective spin model. To summarize our main results: (i) Comparing the mean field theory results for the ground state energy and static spin structure factor with exact diagonalization studies on small clusters, we show that the mean field theory provides a good description of the ground state of the spin model in Eq. (2). (ii) We show that the experimental magnon dispersion is well reproduced by our approach for Hubbard model parameters $U \approx 2.34\text{eV}$, and $t \approx 360\text{meV}$. These parameter values are in reasonable agreement with the experimental estimates⁴ of U , and electronic structure calculations⁵ for t . Our best fit parameters lead to values for the staggered magnetization $m_s \approx 0.285$, spin wave velocity $c \approx 800 \text{ meV}\text{-}\text{\AA}$, and spin stiffness $\rho_s \approx 24\text{meV}$ that are consistent with experimental findings.⁸ Our estimated ratio $U/t \approx 6.5$ is in rough agreement with the value inferred from quantum Monte Carlo (QMC) calculations of Sengupta *et al.*,⁶ though we do not resort to the single mode approximation used by these authors. It is however somewhat smaller than the ratio $U/t \approx 8.8$ obtained from a recent series expansion study of the Hubbard model⁷. (iii) Turning to the spin excitation spectrum beyond the magnon, we find that, along the zone boundary, the spectral weight in the continuum is about 40% of the total spectral weight. In addition, we show that the dynamical spin structure factor exhibits secondary peaks within the mean field theory. It is possible that these features could be explored in neutron scattering experiments with higher resolution and intensity in the near future.

II. EFFECTIVE SPIN MODEL

The effective spin model describing the strong coupling regime of the Hubbard model in (1) takes the form

$$H_{\text{spin}} = \frac{1}{2} \sum_{i,j} J(\mathbf{r}_i - \mathbf{r}_j) \vec{S}_i \cdot \vec{S}_j + \sum_{\square} J_{\square} \left[(\vec{S}_1 \cdot \vec{S}_2)(\vec{S}_3 \cdot \vec{S}_4) + (\vec{S}_1 \cdot \vec{S}_4)(\vec{S}_2 \cdot \vec{S}_3) - (\vec{S}_1 \cdot \vec{S}_3)(\vec{S}_2 \cdot \vec{S}_4) \right]. \quad (2)$$

Here, \vec{S}_i are spin-half operators, and J_{\square} refers to an elementary plaquette on the square lattice with 1–4 labeling sites on its corners. The explicit expressions for the exchange couplings in terms of the Hubbard model parameters are³,

$$J_1 = J_{\hat{x}} = J_{\hat{y}} = 4 \frac{t^2}{U} - 24 \frac{t^4}{U^3} \quad (3)$$

$$J_2 = J_{\hat{x}+\hat{y}} = J_{\hat{x}-\hat{y}} = 4 \frac{t^4}{U^3} \quad (4)$$

$$J_3 = J_{2\hat{x}} = J_{2\hat{y}} = 4 \frac{t^4}{U^3} \quad (5)$$

$$J_{\square} = 80 \frac{t^4}{U^3} \quad (6)$$

With hopping matrix elements between further neighbor sites in the Hubbard model, we expect additional couplings in the effective spin Hamiltonian. However, electronic structure calculations⁵ suggest that these matrix elements are small in magnitude for La_2CuO_4 , so we will not consider them here.

III. SCHWINGER BOSON MEAN FIELD THEORY

To study the ground state and excitations of H_{spin} , we follow ref. 9 and represent spins using two species of bosons $b_{1,2}$ as

$$\vec{S}_i = b_{i\alpha}^{\dagger} \vec{\sigma}_{\alpha\beta} b_{i\beta} \quad (7)$$

with the constraint

$$b_{i\alpha}^{\dagger} b_{i\alpha} = 2S \quad (8)$$

on the boson number at each site. The $\vec{\sigma}$ are Pauli matrices, the spin $S = 1/2$ for our system and, unless specified, the summation over repeated Greek indices is implied here and below. The Hamiltonian can be reexpressed in terms of the bosons by using the identity

$$\vec{S}_i \cdot \vec{S}_j =: B_{ij}^{\dagger} B_{ij} : - A_{ij}^{\dagger} A_{ij} \quad (9)$$

where the bond operators are

$$B_{ij} = \frac{1}{2} b_{i\alpha}^{\dagger} b_{j\alpha} \quad (10)$$

$$A_{ij} = \frac{1}{2} (b_{i,1} b_{j,2} - b_{i,2} b_{j,1}). \quad (11)$$

In the exact Schwinger boson representation, the Hamiltonian obtained using the above identity consists

of 4-boson and 8-boson operators, and one has in addition to deal with the boson number constraint (8). In order to make progress we can resort to a mean field approach. Applied to the Hamiltonian H_{spin} in Eq.2, this consists of three approximations.

(i) First, we reduce the 4-spin interactions to effective 2-spin terms by setting

$$(\vec{S}_1 \cdot \vec{S}_2)(\vec{S}_3 \cdot \vec{S}_4) \rightarrow \langle (\vec{S}_1 \cdot \vec{S}_2) \rangle (\vec{S}_3 \cdot \vec{S}_4) \quad (12)$$

$$+ (\vec{S}_1 \cdot \vec{S}_2) \langle (\vec{S}_3 \cdot \vec{S}_4) \rangle \quad (13)$$

$$- \langle (\vec{S}_1 \cdot \vec{S}_2) \rangle \langle (\vec{S}_3 \cdot \vec{S}_4) \rangle. \quad (14)$$

This renormalizes the two-spin exchange couplings $J(\mathbf{r}_i - \mathbf{r}_j) \rightarrow J^{\text{eff}}(\mathbf{r}_i - \mathbf{r}_j)$ in H_{spin} . It is straightforward to show that $J_1^{\text{eff}} = J_1 + 2J_{\square} \langle \vec{S}_i \cdot \vec{S}_j \rangle$ where ij are nearest neighbor spins, $J_2^{\text{eff}} = J_2 - J_{\square} \langle \vec{S}_i \cdot \vec{S}_m \rangle$ where im are next nearest neighbors, and $J_3^{\text{eff}} = J_3$. At this stage, we obtain a Heisenberg spin Hamiltonian $H_{\text{spin}}^{\text{mf}}$ with only two-spin interactions.

(ii) Next, we do a mean field decoupling of the 4-boson terms arising from the effective two-spin interactions, setting : $B_{ij}^{\dagger} B_{ij} := \langle B_{ij}^{\dagger} \rangle B_{ij} + B_{ij}^{\dagger} \langle B_{ij} \rangle - \langle B_{ij}^{\dagger} \rangle \langle B_{ij} \rangle$ and similarly for $A_{ij}^{\dagger} A_{ij}$. This reduces the spin Hamiltonian $H_{\text{spin}}^{\text{mf}}$ to a quadratic bosonic Hamiltonian $H_{\text{boson}}^{\text{eff}}$.

(iii) Finally, we take the constraint (8) into account using a site-independent Lagrange multiplier λ , thus working with the Hamiltonian $H_{\text{boson}}^{\text{mf}} = H_{\text{boson}}^{\text{eff}} - \lambda \sum_i (b_{i\alpha}^{\dagger} b_{i\alpha} - 2S)$.

The Hamiltonian $H_{\text{boson}}^{\text{mf}}$ is quadratic in the boson fields, and can be diagonalized by a Bogoliubov rotation

$$b_{\mathbf{k},1} = u_{\mathbf{k}} f_{\mathbf{k}\uparrow} - v_{\mathbf{k}} f_{-\mathbf{k}\downarrow}^{\dagger} \quad (15)$$

$$b_{-\mathbf{k},2}^{\dagger} = -v_{\mathbf{k}}^* f_{\mathbf{k}\uparrow} + u_{\mathbf{k}}^* f_{-\mathbf{k}\downarrow}^{\dagger}. \quad (16)$$

Defining

$$\beta_{\mathbf{k}} = \sum_{\mathbf{r}} J^{\text{eff}}(\mathbf{r}) B(\mathbf{r}) \cos(\mathbf{k} \cdot \mathbf{r}) \quad (17)$$

$$\alpha_{\mathbf{k}} = \sum_{\mathbf{r}} J^{\text{eff}}(\mathbf{r}) A(\mathbf{r}) e^{-i\mathbf{k} \cdot \mathbf{r}} \quad (18)$$

$$A(\mathbf{k}) = \sum_{\mathbf{r}} A(\mathbf{r}) e^{i\mathbf{k} \cdot \mathbf{r}} \quad (19)$$

$$B(\mathbf{k}) = \sum_{\mathbf{r}} B(\mathbf{r}) e^{i\mathbf{k} \cdot \mathbf{r}}, \quad (20)$$

and choosing

$$\Omega_{\mathbf{k}} = \sqrt{|\beta_{\mathbf{k}} - \lambda|^2 - |\alpha_{\mathbf{k}}|^2} \quad (21)$$

$$u_{\mathbf{k}} = \cosh(\theta_{\mathbf{k}}) e^{-i\gamma_{\mathbf{k}}} \quad (22)$$

$$v_{\mathbf{k}} = \sinh(\theta_{\mathbf{k}}) e^{-i\gamma_{\mathbf{k}}} \quad (23)$$

$$\cosh(2\theta_{\mathbf{k}}) = |\beta_{\mathbf{k}} - \lambda| / \Omega_{\mathbf{k}} \quad (24)$$

$$\sinh(2\theta_{\mathbf{k}}) = |\alpha_{\mathbf{k}}| / \Omega_{\mathbf{k}}. \quad (25)$$

we arrive at the diagonal form

$$H_{\text{boson}}^{\text{mf}} = \frac{1}{2} \sum_{\mathbf{k},\mu} \Omega_{\mathbf{k}} f_{\mathbf{k},\mu}^{\dagger} f_{\mathbf{k},\mu} + \lambda (S + 1/2) N_{\text{site}}$$

$$- \frac{1}{2} \sum_{\mathbf{k}} \beta(\mathbf{k}) + \frac{1}{2} \sum_{\mathbf{k}} (A^*(\mathbf{k}) \alpha_{\mathbf{k}} - B^*(\mathbf{k}) \beta_{\mathbf{k}}) \quad (26)$$

The f -particles appearing here are bosonic $S = 1/2$ spinons.

The above parameters $u_{\mathbf{k}}, v_{\mathbf{k}}$ depend on the mean field values of $\langle B_{ij} \rangle \equiv B(\mathbf{r})$, $\langle A_{ij} \rangle \equiv A(\mathbf{r})$, and $\langle \vec{S}_i \cdot \vec{S}_j \rangle$ appearing in the quadratic Hamiltonian. These mean field parameters are evaluated in the ground state of (26), which results in a self-consistent theory. For completeness, the self consistency conditions and the constraint equation are given by

$$A(\mathbf{k}) = \frac{\alpha(\mathbf{k})}{2\Omega_{\mathbf{k}}} \quad (27)$$

$$B(\mathbf{k}) = \frac{\beta_{\mathbf{k}} - \lambda}{2\Omega_{\mathbf{k}}} - \frac{1}{2} \quad (28)$$

$$2S + 1 = \frac{1}{N_{site}} \sum_{\mathbf{k}} \frac{\beta_{\mathbf{k}} - \lambda}{\Omega_{\mathbf{k}}} \quad (29)$$

It is well known⁹ that long-range magnetic order appears in this formulation if the energy $\Omega_{\mathbf{k},\mu}$ vanishes at some wavevector(s) $\mathbf{k} = \{\mathbf{Q}_i\}$ in the thermodynamic limit, leading to condensation of the spinons at these momenta. In the Néel state on the square lattice, the spinons condense at wavevectors $\mathbf{Q} = \pm(\pi/2, \pi/2)$ in the thermodynamic limit¹⁰ leading to magnetic order at the wavevector connecting these points, namely (π, π) . We report below the ground state properties of the model with four-spin interactions, and present a comparison with exact diagonalization results on small clusters.

IV. GROUND STATE PROPERTIES

A. Comparison with exact diagonalization results on small clusters

Schwinger boson mean field theory provides very accurate results for the ground state properties of the nearest-neighbor Heisenberg antiferromagnet⁹. In order to assess the accuracy of this approximation scheme in presence of the four-spin interaction term it is useful to compare the mean field estimates of ground state properties with exact diagonalization numerics. To this end, we have performed Lanczos exact diagonalizations of the spin Hamiltonian (2) on the 4×4 , $\sqrt{20} \times \sqrt{20}$, $\sqrt{32} \times \sqrt{32}$ and 6×6 clusters. In particular we have focused on exchange interactions corresponding to $U/t \rightarrow \infty$ (the Heisenberg limit), and $U/t = 6.5$, for which the mean field theory fits the experimental magnon dispersion of La_2CuO_4 as discussed in the next section. The latter choice of U/t corresponds to $J_2 = J_3 = 0.0276J_1$ and $J_{\square} = 0.55J_1$ in (2).

We have calculated the ground state energy and the static spin structure factor $S(\mathbf{q})$

$$S(\mathbf{q}) = \sum_j \langle \tilde{S}(\mathbf{r}_j) \cdot \tilde{S}(\mathbf{r}_0) \rangle e^{-i\mathbf{q} \cdot (\mathbf{r}_j - \mathbf{r}_0)} \quad (30)$$

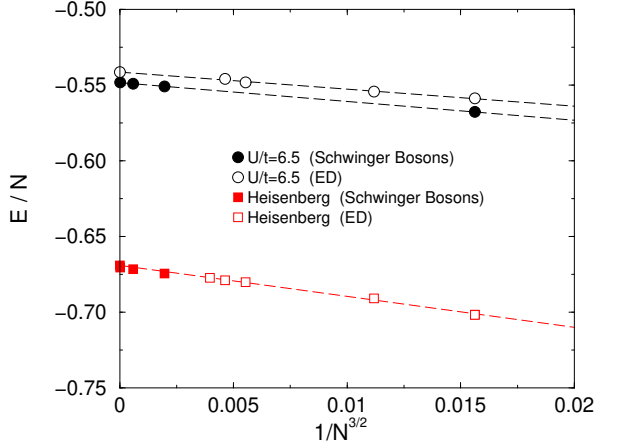


FIG. 1: Comparison of Schwinger boson mean field theory and exact diagonalization calculations of the ground state energy per site for the spin model in Eq. (2) for the Heisenberg limit ($U/t \rightarrow \infty$) and for $U/t = 6.5$.

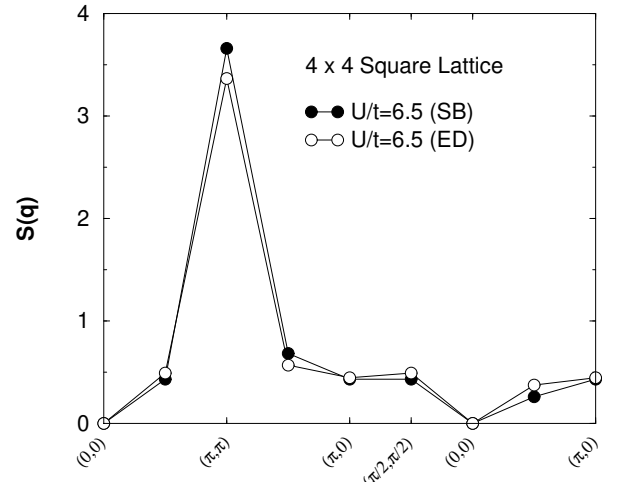


FIG. 2: Comparison of Schwinger boson mean field theory and exact diagonalization calculations of the static spin structure factor $S(\mathbf{q})$ on a 4×4 lattice. The renormalization effects on the spin operators at finite U/t have been taken into account through Eq.(31).

In Eq. (30) above, we have taken into account that the spin operator of the Hubbard model is transformed under the same unitary transformation which enables us to work with the effective spin model of Eq. (2). Specifically,

$$\tilde{S}(\mathbf{r}) = \vec{S}(\mathbf{r}) \left(1 - 2 \frac{t^2}{U^2}\right) + \frac{t^2}{U^2} \sum_{\delta=\pm\hat{x},\pm\hat{y}} \vec{S}(\mathbf{r} + \delta), \quad (31)$$

as also noted by Delannoy *et al.*¹¹ The results presented in Figs. 1 and 2 clearly show that the Schwinger boson

approach is still rather accurate even for a moderate interaction strength $U/t = 6.5$. We next turn to the staggered magnetization and spin stiffness in the thermodynamic limit for the model (2).

B. Staggered magnetization and spin stiffness in the thermodynamic limit

From finite-size scaling of the static structure factor in Eq. (30) we obtain the antiferromagnetic order parameter m_s given by

$$m_s^2 = \lim_{N_{\text{site}} \rightarrow \infty} \frac{S(\pi, \pi)}{N_{\text{site}}}. \quad (32)$$

We find that the staggered magnetization for $U/t = 6.5$ extrapolates, within Schwinger boson mean field theory, to $m_s \approx 0.285$, slightly smaller than that for the nearest-neighbor Heisenberg model ($m_s^{nn} \approx 0.303$). This decrease of the staggered magnetization is due to $\mathcal{O}(t/U)^2$ corrections to the spin operator in Eq. (31), which reflects local charge fluctuations in the insulator as pointed out in Ref. 11.

Following Stringari¹², we extract the spin stiffness from the small momentum behavior of the structure factor. Specifically, approaching the magnetically ordered state in a rotationally invariant formulation, the static structure factor for small q is related to the spin stiffness through

$$\rho_s = \frac{cS(\mathbf{q} \rightarrow 0)}{q} \quad (33)$$

where c is the spin wave velocity of the linearly dispersing magnon at momenta near $(0, 0)$ and (π, π) . The spin-wave velocity c can be obtained from the magnon dispersion as discussed in connection with the excitation spectrum in the next section. This, together with the calculated structure factor in the limit, $\mathbf{q} \rightarrow 0$, yields the spin stiffness through Eq. (33). As discussed in detail in the next section, a fit to the overall magnon dispersion in La_2CuO_4 yields a spin wave velocity $c \approx 800\text{meV}\text{-}\text{\AA}$. Assuming a lattice spacing 3.85\AA for the CuO_2 plane, this yields $\rho_s \approx 24\text{meV}$, which is consistent with experimental findings.⁸ Note that the spin stiffness can also be obtained by studying the change in ground state energy for a slowly varying spin twist.

V. EXCITATION SPECTRUM

To probe the spectrum of $S = 1$ excitations at a given momentum \mathbf{q} , which is of interest for neutron scattering experiments, one can act with the operator $S^+(\mathbf{q}) = \sum_{\mathbf{k}} b_{\mathbf{k},1}^\dagger b_{\mathbf{k}-\mathbf{q},2}$. Making a Bogoliubov rotation to spinon variables, we can rewrite this as

$$S^+(\mathbf{q}) = G(\mathbf{q}) \sum_{\mathbf{k}} (u_{\mathbf{k}} f_{\mathbf{k}\uparrow} - v_{\mathbf{k}} f_{-\mathbf{k}\downarrow}^\dagger)$$

$$\times (u_{\mathbf{k}-\mathbf{q}} f_{\mathbf{k}-\mathbf{q}\uparrow} - v_{\mathbf{k}-\mathbf{q}} f_{-\mathbf{k}+\mathbf{q}\downarrow}^\dagger) \quad (34)$$

where the additional “form factor”

$$G(\mathbf{q}) = 1 - \frac{t^2}{U^2} (2 - \cos q_x - \cos q_y) \quad (35)$$

arises from the transformation of the spin operator according to Eq. (31).

We see that at a given momentum \mathbf{q} , if one of the two spinons combining to give the spin operator is condensed (which would happen for spinon momenta $\pm(\pi/2, \pi/2)$ in the Néel state), that part behaves as a single particle excitation with a well defined dispersion - this is the magnon. For general \mathbf{k} , both spinons are uncondensed and this remainder of the sum contributes to the scattering continuum. Quite generally, both parts play a role when we evaluate the spectral function for the $S^+(\mathbf{q})$ operator.

A. Magnon dispersion

From the above discussion, it is clear that the magnon energy at momentum \mathbf{q} within the mean field theory of the Néel state is just given by $\Omega_{\mathbf{Q}-\mathbf{q}}/2$ where $\mathbf{Q} = \pm(\pi/2, \pi/2)$. For our choice of mean field decoupling, and for spin $S \rightarrow \infty$, this is exactly half the value given by spin-wave theory¹⁵. It is known¹⁶ that Schwinger boson mean field theory for the Heisenberg model has this shortcoming, which can be fixed by working within a large- N generalization of the Schwinger boson theory and including $1/N$ corrections to the mean field ($N = \infty$) result. Since we reduce our original Hamiltonian in Eq. (2) to an effective Heisenberg-type model before we use the Schwinger boson representation, we expect the same fluctuation corrections to appear in our case as well, however an explicit calculation is beyond the scope of this paper. Here and below we will work with $\Omega_{\mathbf{k}}$ as the magnon energy. Note that the $\mathcal{O}(t/U)^2$ corrections to the spin operator do not affect the magnon dispersion.

Fig. 3 shows the magnon energy $\Omega_{\mathbf{k}}$ obtained within the mean field theory for $U/t = 6.5$ and $t = 360\text{meV}$ compared with the experimental data from Coldea *et al.* This choice of parameters gives a good fit to the dispersion over the entire contour along the Brillouin zone, including both the linearly dispersing spin-wave regime as well as the high energy magnon dispersion along the zone boundary. While the fit along the zone boundary is easy to see in the figure, its accuracy at low energies may be seen from the spin wave velocity in the mean field theory $c \approx 800\text{meV}\text{-}\text{\AA}$ being in good agreement with experiment. We also point out that at much larger values of U/t ($\gtrsim 7$), we are unable to reproduce properly the dip in the magnon dispersion at $(\pi/2, \pi/2)$ while traversing the zone boundary. While further neighbor hoppings in the Hubbard model (e.g. third-nearest neighbor hopping t_3) could produce a similar dip near $(\pi/2, \pi/2)$ by generating an antiferromagnetic exchange of order t_3^2/U , electronic structure calculations for La_2CuO_4 indicate that

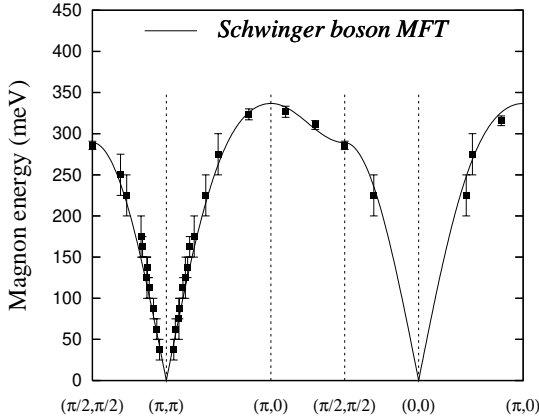


FIG. 3: Fit of the magnon dispersion obtained from Schwinger boson mean field theory to the experimental data at $T = 10K$ in Ref. 2 along the standard contour in the Brillouin zone. The Hubbard model parameters used for this fit are $t = 360\text{meV}$ and $U = 2.34\text{eV}$, with the effective spin Hamiltonian couplings given by Eq. (6).

such hopping matrix elements are too small to produce the measured dip.

Qualitatively similar results have been obtained by other workers within diagrammatic treatments of the Hubbard model¹³, or treating the Hamiltonian with multispin exchange interactions using Dyson-Maleev bosons¹⁴ to represent the spins. However, the latter authors do not attempt to connect the effective spin model to a microscopic electronic Hamiltonian, and they obtain exchange couplings quite different from our estimates.

B. Scattering continuum

Having fixed the parameter values U, t from fitting the magnon dispersion to the data, we next turn to the scattering continuum. Specifically, we are interested in asking how much weight is present in the continuum relative to the magnon, and if there are any features in the continuum which may be experimentally observable. Recall that in the mean field theory this part of the spectrum is just the two-spinon excitation continuum.

In order to obtain the weight in the continuum versus the magnon, we consider the spectral weight integrated over energy. This is just the structure factor

$$S(\mathbf{q}) = G^2(\mathbf{q}) \sum_{\mathbf{k}} \left[\left(\frac{|\beta_{\mathbf{k}-\mathbf{q}} - \lambda|}{\Omega_{\mathbf{k}-\mathbf{q}}} - 1 \right) \left(\frac{|\beta_{\mathbf{k}} - \lambda|}{\Omega_{\mathbf{k}}} + 1 \right) - \frac{\alpha_{\mathbf{k}}^* \alpha_{\mathbf{k}-\mathbf{q}}}{\Omega_{\mathbf{k}} \Omega_{\mathbf{k}-\mathbf{q}}} \right] \quad (36)$$

To obtain the magnon weight part, we need to keep only

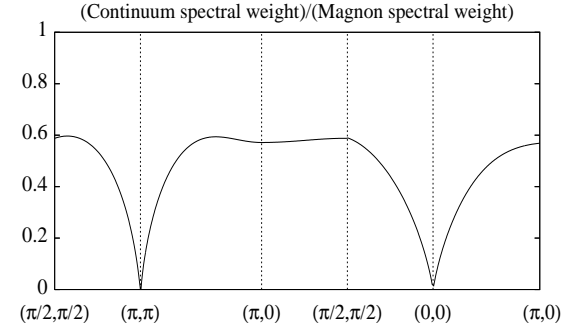


FIG. 4: Ratio of continuum and magnon spectral weights along a contour in the Brillouin zone. The magnon exhausts the spectral weight for $\mathbf{q} \rightarrow (0, 0)$ and $\mathbf{q} \rightarrow (\pi, \pi)$ consistent with general arguments¹². Along the zone boundary, the continuum accounts for nearly 40% of the total spectral weight.

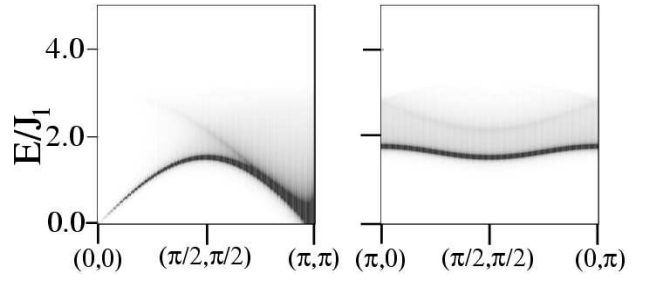


FIG. 5: Grayscale plot of the dynamical structure factor $S(\mathbf{q}, E)$ of the spin model (2) with optimal parameters as in Fig. 1, with high intensity in black. The gray areas indicate regions of continuum scattering. The intensity has been scaled to clearly show both the magnon and secondary peak features. Left panel: Magnon peak and the single secondary peak along $(0, 0) \rightarrow (\pi, \pi)$. The magnon and secondary peak intensities vanish as $\mathbf{q} \rightarrow (0, 0)$. Right panel: Magnon peak and two secondary peaks along the zone boundary $(\pi, 0) \rightarrow (0, \pi)$. The two secondary peaks merge at $(0, \pi)$ and $(\pi, 0)$. The dip in the magnon dispersion at $(\pi/2, \pi/2)$ is clearly visible.

those contributions where $\Omega_{\mathbf{k}}$ or $\Omega_{\mathbf{k}-\mathbf{q}}$ would vanish in the thermodynamic limit (or are minimum on a finite but large lattice). The continuum contribution is the remaining part of the sum. In Fig. 4 we plot the ratio of these weights over the same contour in the Brillouin zone over which the magnon dispersion is displayed. This ratio is of course insensitive to the “form factor” $G(\mathbf{q})$, however the important thing to note from the plot is that the continuum weight is most significant along the zone boundary and accounts for nearly 40% of the total spectral weight. This is the most promising region to study the continuum in neutron scattering experiments.

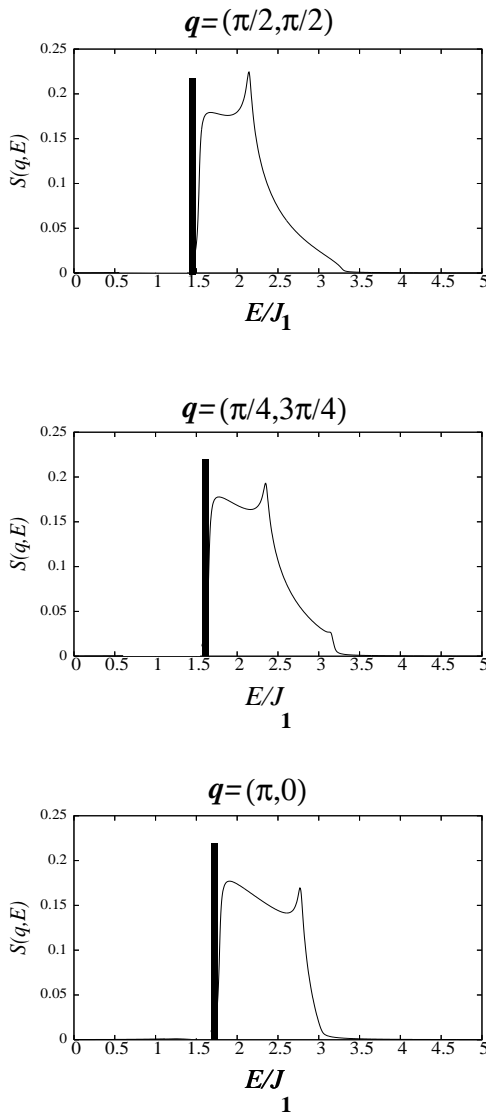


FIG. 6: The dynamical structure factor along the zone boundary at $(\pi/2, \pi/2)$ (top), $(\pi/4, 3\pi/4)$ (middle) and $(\pi, 0)$ (bottom), showing the sharp magnon (as a bold vertical line not drawn to scale) and the broad continuum including the sharp secondary features most clearly visible at $(\pi/4, 3\pi/4)$.

The continuum weight is also considerable along the line from $(\pi, 0)$ to $(\pi, \pi/2)$.

In order to display possible interesting features in the continuum scattering we have plotted the spectrum of excitations at a few \mathbf{q} points along the zone boundary in

Fig. 6, as well a grayscale plot of the spectral function in Fig. 5 along $(0, 0) \rightarrow (\pi, \pi)$ and along $(\pi, 0) \rightarrow (0, \pi)$. We see that in addition to the magnon, there are singular secondary features in the spectrum. These secondary peaks can be shown to arise from special points $\{\mathbf{K}\}$ in the Brillouin zone in the vicinity of which the sum $\Omega_{\mathbf{k}} + \Omega_{\mathbf{k}-\mathbf{q}}$ varies slowly (dispersing as $\sim |\mathbf{k}-\mathbf{K}|^4$) giving rise to a log singular density of states for the two-spinon continuum.

These secondary peaks and continuum scattering also arise within the mean field theory for the nearest neighbor Heisenberg model, with minor quantitative changes due to differences in the spinon dispersion. The effect of fluctuations beyond the mean field result on the magnon dispersion and the scattering continuum is beyond the scope of this paper, and is currently being investigated.

VI. CONCLUDING REMARKS

We have presented a Schwinger boson mean field description of the effect of four-spin interactions on spin dynamics in Mott insulators. Such multispin interactions and their effects are potentially important in correlated insulators with local charge fluctuations. For La_2CuO_4 , the experimental magnon dispersion is well reproduced by our approach with Hubbard model parameters $U \approx 2.34\text{eV}$, and $t \approx 360\text{meV}$. These values are in consistent with experimental estimates⁴ and electronic structure calculations⁵. This leads to a sizeable value of the ring-exchange term $J_{\square} \approx 0.55J_1$ in the effective spin Hamiltonian. Good agreement with experiments is also obtained for the staggered magnetization, spin wave velocity, and spin stiffness, thus leading to a consistent description of the magnetic behavior of this Mott insulator. Beyond the single magnon excitation, we have shown that there is considerable spectral weight in the continuum along the zone boundary, and that the dynamical structure factor exhibits secondary peaks which we understand as arising from the density of states of two-spinon excitations. These could be explored in experiments with high intensity neutron sources in the near future.

Acknowledgments

We thank Radu Coldea and Gregoire Misguich for useful discussions and correspondence, and Anton Burkov for a stimulating conversation. AP acknowledges support through grant DOE LDRD DEAC03-76SF00098.

¹ D.J. Thouless, Proc. Phys. Soc. (London) **86** 893 (1965); M. Roger, J.H. Hetherington, and J.M. Delrieu, Rev. Mod. Phys. **55** 1 (1983); M. Siqueira, J. Nyeki, B. Cowan and

J. Saunders, Phys. Rev. Lett. **78**, 2600 (1997); B. Bernu, L. Candido, and D.M. Ceperley, Phys. Rev. Lett. **86**, 870 (2001);

- ² R. Coldea, S.M. Hayden, G. Aeppli, T.G. Perring, C.D. Frost, T.E. Mason, S.-W.Cheong, and Z. Fisk, Phys. Rev. Lett. **86**, 5377 (2001).
- ³ A. H. MacDonald, S. M. Girvin, and D. Yoshioka, Phys. Rev. B **41**, 2565 (1990).
- ⁴ S.L. Cooper, G.A. Thomas, A.J. Millis, P.E. Sulewski, J. Orenstein, D.H. Rapkine, S.-W. Cheong and P.L. Trevor, Phys. Rev. B **42**, 10785 (1990); Y. Tokura, Y. Koshihara, T. Arima, H. Takagi, S. Ishibashi, T. Ido and S. Uchida, Phys. Rev. B **11657** (1990).
- ⁵ E. Pavarini, I. Dasgupta, T. Saha-Dasgupta, O. Jepsen and O.K. Andersen, Phys. Rev. Lett. **87**, 047003 (2001).
- ⁶ P. Sengupta, R. Scalettar, R.R.P Singh, Phys. Rev. B **66**, 144420 (2002).
- ⁷ W. Zheng, R.R.P. Singh, J. Oitmaa, O.P. Sushkov and C.J. Hamer, cond-mat/0501029 (unpublished).
- ⁸ K. Yamada, K. Kakurai, Y. Endoh, T.R. Thurston, M.A. Kastner, R.J. Birgeneau, G. Shirane, Y. Hidaka, and T. Murakami, Phys. Rev. B **40**, 4557 (1989); B. Keimer, N. Belk, R.J. Birgeneau, A. Cassanho, C.Y. Chen, M. Greven, M.A. Kastner, A. Aharony, Y. Endoh, and R.W. Erwin, Phys. Rev. B **46**, 14034 (1992).
- ⁹ D.P. Arovas and A. Auerbach, Phys. Rev. B **38**, 316 (1988); H.A. Ceccatto, C.J. Gazza, and A.E. Trumper, Phys. Rev. B **47**, 12329 (1993); for an excellent review see also: G. Misguich, Ph.D. thesis, Université Paris 6 (1999), in French.
- ¹⁰ This is for our particular mean field decoupling. The spinon dispersion is not a gauge invariant quantity, although the number of gapless wavevectors and the momentum difference between them are gauge invariant.
- ¹¹ J.-Y.P. Delannoy, M.J.P. Gingras, P.C.W. Holdsworth and A.-M.S. Tremblay, cond-mat/0412033 (unpublished).
- ¹² S. Stringari, Phys. Rev. B **49**, 6710 (1994).
- ¹³ N.M.R. Peres and M.A.N. Araújo, Phys. Rev. B **65**, 132404 (2002).
- ¹⁴ A. Katanin and A. Kampf, Phys. Rev. B **66**, 100403 (2002).
- ¹⁵ P.W. Anderson, Phys. Rev. **86**, 694 (1952).
- ¹⁶ See A. Auerbach, “*Interacting Electrons and Quantum Magnetism*”, Springer-Verlag (1994). For the mean field decoupling scheme in this book and in some earlier papers, the static structure factor and the correction to the classical ground state energy come out different by a factor of 3/2 and 2 respectively at large- S compared with spin-wave theory. By contrast, our mean field decoupling gives accurate ground state properties (structure factor and energy) but a factor-of-two difference appears in the magnon dispersion.